DOI: 10.5604/01.3001.0015.4795

Volume 108 • Issue 1 • September 2021

Journal of Achievements in Materials and Manufacturing Engineering

International Scientific Journal published monthly by the World Academy of Materials and Manufacturing Engineering

Bearing capacity of embedded and skirted E-shaped footing on layered sand

S. Nazeer [a], R.K. Dutta [b,*]

[a] PG Student, Department of Civil Engineering, National Institute of Technology, Hamirpur, India

[b] Professor, Department of Civil Engineering, National Institute of Technology, Hamirpur, India

* Corresponding e-mail address: rkd@nith.ac.in

ORCID identifier: https://orcid.org/0000-0002-4611-9950 (R.K.D.)

ABSTRACT

Purpose: The purpose of this study is to investigate the ultimate bearing capacity of the embedded and skirted E-shaped footing resting on two layered sand using finite element method. The analysis was carried out by using ABACUS software.

Design/methodology/approach: The numerical study of the ultimate bearing capacity of the embedded and skirted E-shaped footing resting on layered sand and subjected to vertical load was carried out using finite element analysis. The layered sand was having an upper layer of loose sand of thickness H and lower layer was considered as dense sand of infinite depth. The various parameters varied were the friction angle of the upper (30° to 34°) and lower (42° to 46°) layer of sand, the skirt depth (0B, 0.25B, 0.5B and 1B), the embedment depth (0B, 0.25B, 0.5B and 1B) and the thickness (0.5B, 2B and 4B) of the upper sand layer, where B is the width of the square footing.

Findings: The ultimate bearing capacity was higher for the skirted E-shaped footing followed by embedded E-shaped footing and unskirted E-shaped footing in this order for all combinations of variables studied. The improvement in the ultimate bearing capacity for the skirted E-shaped footing in comparison to the embedded E-shaped footing was in the range of 0.31 % to 61.13 %, 30.5 % to 146.31 % and 73.26 % to 282.38% corresponding to H/B ratios of 0.5, 2.0 and 4.0 respectively. The highest increase (283.38 %) was observed at $\varphi 1$ =30° and $\varphi 2$ =46° corresponding to H/B and Ds/B ratio of 4.0 and 1.0 respectively while the increase was lowest (0.31 %) at $\varphi 1$ =34° and $\varphi 2$ =46° at H/B ratio of 0.5 and Ds/B ratio of 0.5. For the skirted E-shaped footing, the lateral spread was more as in comparison to the embedded E-shaped footing. The bearing capacity of the skirted footing was equal the sum of bearing capacity of the surface footing, the skin resistance developed around the skirt surfaces and tip resistance of the skirt with coefficient of determination as 0.8739. The highest displacement was found below the unskirted and embedded E-shaped footing, and at the skirt tip in the case of the skirted E-shaped footing. Further, the displacement contours generated supports the observations of the multi-edge embedded and skirted footings regarding the ultimate bearing capacity on layered sands.

Research limitations/implications: The results presented in this paper were based on the numerical study conducted on E shaped footing made from a square footing of size 1.5 m x 1.5 m. However, further validation of the results presented in this paper, is recommended using experimental study conducted on similar size E shaped footing.

Practical implications: The proposed numerical study can be an advantage for the architects designing similar types of super structures requiring similar shaped footings.

Originality/value: No numerical study on embedded and skirted E shaped footing resting on layered sand (loose over dense) were conducted so far. Hence, an attempt was made in this article to estimate the bearing capacity of the same footings.

Keywords: Skirted and embedded E-shaped footing, Finite element analysis, Bearing capacity, Layered sand, Skirt depth, Embedment depth, Thickness of upper layer, Friction angle

Reference to this paper should be given in the following way:

S. Nazeer, R.K. Dutta, Bearing capacity of embedded and skirted E-shaped footing on layered sand, Journal of Achievements in Materials and Manufacturing Engineering 108/1 (2021) 5-23. DOI: https://doi.org/10.5604/01.3001.0015.4795

1. Introduction

Common footing shapes, such as rectangle, strip, circular, or ring, have been used in footing design for a long time. Unusual geometries may be used for the design in some cases due to static, architectural, and economic requirements. Footings with more than four edges are referred to as multi-edge footings. These footings are designed to safely and economically transfer the load from the irregularly shaped structure to the underlying soils. Furthermore, it is well known that a footing resting on loose sand will experience shear failure followed by a substantial settlement. Densification of the sand to a certain depth is carried out in this situation to increase the bearing capacity. Contrary to popular belief, the presence of loose sand over a dense sand layer can sometimes be overlooked due to poor subsurface investigation. In each of the cases above, the effect of the loose sand layer overlying the dense sand layer on the bearing capacity of the footing must be considered. In the literature, there was significant work for traditional shaped footings with and without skirts resting on single or two layered soils [1-35]. These studies found that the geometry of the footing, skirt material property, footing, sand-skirt-footing interface characteristics, and sand relative density all influenced the bearing capacity of the skirted regular footing on sand. Studies were also reported for the embedded footings [2,8,29] as well as on multi-edge skirted footings on a single or two layers of sands [36-43]. In all the above studies the parameters varied were the footing width, relative density of sand, angle of internal friction and skirt depth. The study reported by [37] on a square and a multi-edge H-shaped footing, with and without skirts, concluded that the development of shear zones in between the multi edges leads to passive force generation in other parts and hence more load is needed to extend shear zones in greater areas and thus to bring the soil to failure stage. The authors further concluded that the skirted footings were more effective for the sand with low relative density as compared to the high relative density. The model studies reported by [36] concluded that for the bearing capacity of footing was seen to increase with the change in the condition of the interface from partially rough to rough. A three-dimensional numerical analysis was also reported by [42] on H, T and plus shaped footings placed on reinforced sand to investigate the bearing capacity. Study reported by [38] concluded that the increase in the bearing capacity was higher in doubly skirted hexagonal footing than that of singly skirted footing. The results also revealed that the sand with higher unit weight showed higher increase in the bearing capacity. A numerical study was carried out by [44] on a strip footing subjected to eccentric and inclined loading on a rock mass using the upper and lower bound finite element analysis based on the geological strength index and the yield parameter of the rock. The authors concluded that with the increase in the geological strength index and the yield parameters, the bearing capacity increases. Researchers [45-49] obtained the undrained strength of homogeneous and non-homogeneous clays by finite element analysis for the shallow and deep footings on clay. These studies concluded that the bearing capacity of the clay increased linearly with the increase in the shear strength. It was reported by [8] that the pressure-settlement curves related to the embedded pier foundation plots higher than the surface skirted footings. However, it was reported by [2] that the skirted footing was more beneficial than that of the embedded footing and similar findings were reported by [29]. Thus, from the studies reported above, it can be concluded that skirted footings can be a better and economical means for the enhancement of bearing capacity in regular shaped as well as in multi edge footings. However, very few studies related to multi-edge footings with or without skirts resting on layered sand is available in literature. The skirt and footing material used in the literature for the studies so far was the steel. No studies have been conducted so far for the concrete as the skirt and footing material. Thus, the present study involves the numerical

analysis of embedded and skirted E-shaped footing resting on layered sand in order to fill this gap.

2. Finite element modelling

The present study uses a commercially available ABACUS software. Skirted and embedded E-shaped footing subjected to vertical concentric load resting on loose sand overlying dense sand was used for modelling as shown in Figure 1. The soil was restricted from the horizontal movements and the base was fixed in all the three translational and rotational degrees of freedom. The two layered soil model was created with the minimum dimensions of 5B from footing edge in the x, y and z direction so as to avoid the boundary effects and to stimulate the actual ground conditions as per [41,32]. The depth of skirt or the embedment depth of the footing was varied from 0B to 1B, thickness (H) of the upper loose sand layer was varied from 0.5B to 4B and that of the lower dense sand was considered to be of infinite depth. The soil parameters varied were unit weight of upper loose sand layer (γ_1) and lower dense sand layer (γ_2), friction angle of upper (ϕ_1) and lower (ϕ_2) layer of sand. The modulus of elasticity, Poisson ratio and dilation angle of the upper layer of loose sand (E_1, μ_1, ψ_1) and lower dense sand (E_2, μ_2, ψ_2) layer were considered in this study. The unit weight of the upper loose (γ_1) and lower dense sand layer (γ_2) were varied as 13.5kN/m^3 to 15.0kN/m^3 and 18kN/m^3 to 20 kN/m^3 respectively. The friction angle of the upper loose sand (ϕ_1) and lower dense sand (ϕ_2) layer were varied from 30°to 34° and 42° to 46° respectively. These friction angles were taken corresponding to the unit weight of the sand as per [27]. Modulus of elasticity for the upper loose and lower dense layer of the sand were computed using a formula 1200 (N + 6) kPa as per [50,51]. In this formula, the N stands for standard penetration resistance and its value was taken against the chosen value of friction angle as per [52]. The Poisson's ratio for the upper loose sand and lower dense sand layers were varied from 0.3 to 0.35 and 0.2 to 0.3 as per [50] respectively.

a)

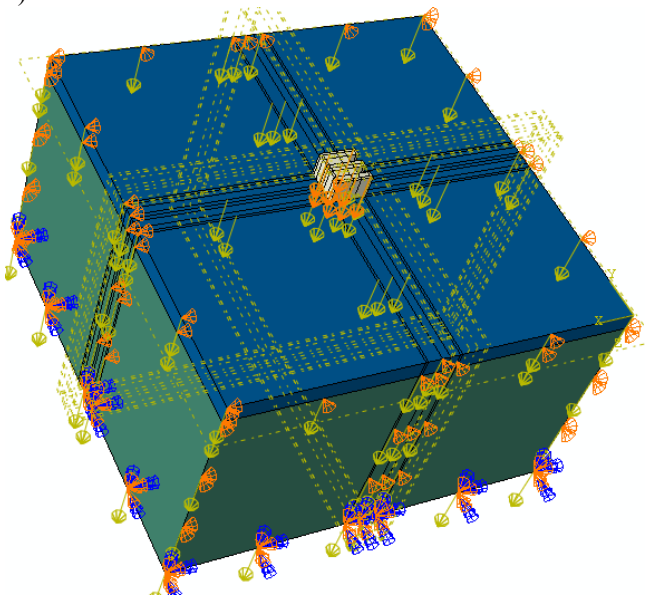

b)

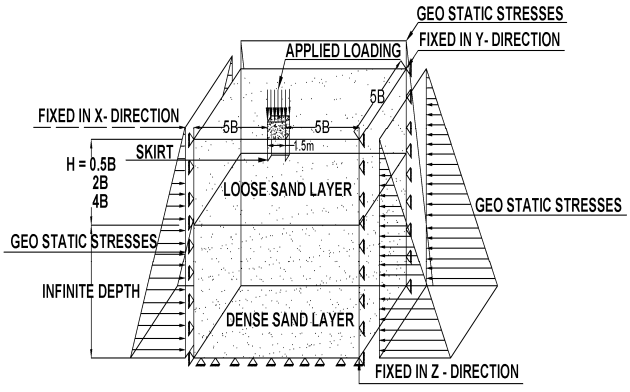

Fig. 1 Skirted and embedded E-shaped footing subjected to a vertical concentric load resting on loose sand overlying dense sand (a) boundary and loading condition (b) schematic representation of loading

Table 1.
Dilation angles used for modelling

Friction angle	Dilation angle
30°	0°
32°	2°
34°	4°
42°	12°
44°	14°
46°	16°

The dilation angle (ψ) for both the layers of sand was calculated as per the equation φ-30° proposed by [53] for modelling and their values are tabulated in Table 1. The density (γ), modulus of elasticity (E) and the Poisson ratio (υ) of the concrete was taken as 24 kN/m^3, 30 GPa and 0.25 respectively for the footing material as per [54,55].

3. Finite element meshing

The dimension of the E-shaped footing for both the skirt and embedded case, considered for modelling was 1.5 m x 1.5 m x1.0 m as per [8] as shown in Figure 2.

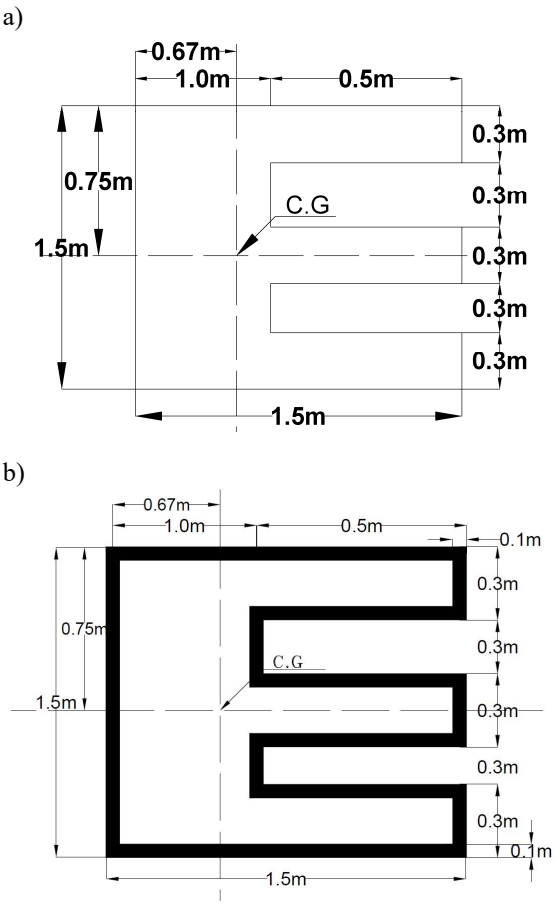

Fig. 2. Location of centre of gravity for E-shaped footing (a) without skirt (b) with skirt

The E-shaped footing was made from the square footing of size 1.5 m x 1.5 m. Skirt thickness was taken as 100 mm as per the minimum thickness reported by [56] for all the case combinations studied. The Mohr-Coulomb model was used for the analysis to simulate the sand behaviour in this study. The Mohr-Coulomb model incorporates five input parameters viz. E and υ for soil elasticity, ϕ and c for soil plasticity and ψ for the soil dilatancy. Hence it forms a typical elastic-perfectly plastic model. Keeping in mind, the complex nature of soil, it is difficult to form exactly accurate stress-deformation plot and then to analyse it. Therefore, the theory of elasticity which is an approximate solution for the soil behaviour is often used [32]. The element used for modelling was C3D8R. Near the vertical axis of the footing, the meshing was finer which changed to coarser as the distance from the footing edge increased as shown in the Figure 3. The initial geostatic stress was also applied before the application of the vertical loading. The footing soil interface was assumed to be rough with the interface coefficient of friction $\tan(\delta)$ = 0.36, 0.39 and 0.42 corresponding to a friction angle of the upper loose sand layer of 30°, 32° and 34° respectively. The convergence study reveals that the optimal number of elements obtained in the present study was **39840**. Beyond this range, there was not an appreciable change in the ultimate bearing capacity of model footings.

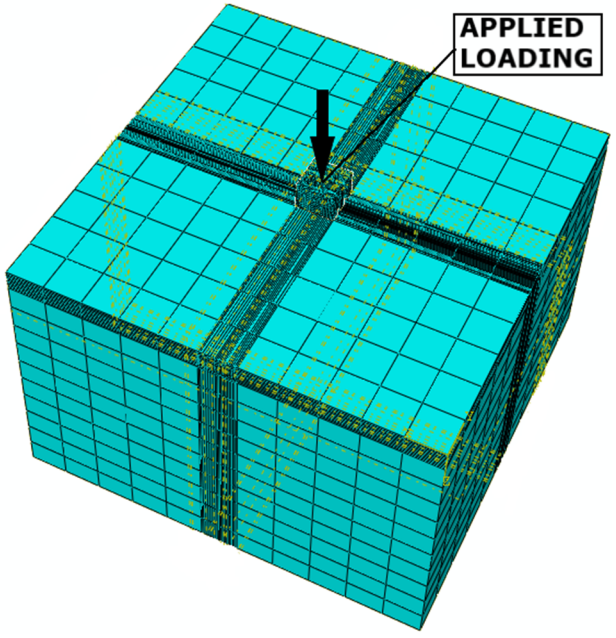

Fig. 3. Meshing of Skirted and Embedded E-shaped footing resting on layered sand

4. Software validation

To validate the software, it was thought to perform an additional analysis using the experimental data for the square footing resting on single layer of sand and reported by [10]. This validation was conducted numerically for square footing the skirt. The soil dimensions were taken as 700 mm x 450 mm x 600 mm and the steel footing of size 50 mm x 50 mm with a thickness of 10mm was used. The skirt depth was varied as 0.25*B*, 0.5*B* and 1*B* with the constant skirt thickness of 5 mm as per [10]. The unit weight of sand corresponding to relative density of 30% was taken

as 13.87 kN/m^3. Friction angle corresponding to the same relative density and unit weight as mentioned above were taken as 36.5°. It is pertinent to mention here that a friction angle obtained through triaxial testing corresponding to a relative density of 30% was 36.06° as reported by [37]. Hence the friction angle of the sand chosen for modelling is justified. The internal friction angle between the steel and soil was taken as 22° corresponding to a relative density of 30% for modelling. The density of steel, modulus of elasticity and Poisson ratio of the footing material were taken as 78.50 kN/m^3, 210 GPa and 0.303 as per [56]. The comparison of the results is shown in Table 2. Study of Table 2 reveals that the average deviation in the bearing capacity was 11.8 % corresponding to the different skirt depths at constant relative density of 30%.

Table 2.
Comparison of the results for the software validation

Bearing capacity (q_u) at s/B ratio of 10%		
D_S/B (R.D = 30%)	Khatri et al [16]	Present work
0.25	42.7	31.9
0.50	89.3	74.6
1.00	186.5	196.4

5. Codification

For easy reference and comprehensibility, specific codification was used in graphs. The codification SE-XX-YY-ZZ was used for representing Skirted/Embedded E-shape footing (S or E) followed by the friction angle of upper loose sand layer (XX represents 30°, 32°, 34°),friction angle of lower dense sand layer (YY represents 42°, 44°, 46°) and H/B ratio (ZZ represents 0.5, 2,4) respectively. However, in case of five variables viz. SE-XX-YY-ZZ-II , ZZ represents the D_s/B ratio and II represents the H/B ratio respectively.

6. Results and discussions

Figure 4 presents the typical pressure-settlement ratio plots obtained from the numerical study. A total of 216 tests were carried out in this numerical analysis. Typically, the reference point for calculating the bearing capacity of the embedded and skirted E-shaped footing was taken at the CG of footing and at the skirt tip level respectively as per [1]. The ultimate bearing capacity was taken corresponding to the peak pressure as per [36]. The numerical study was

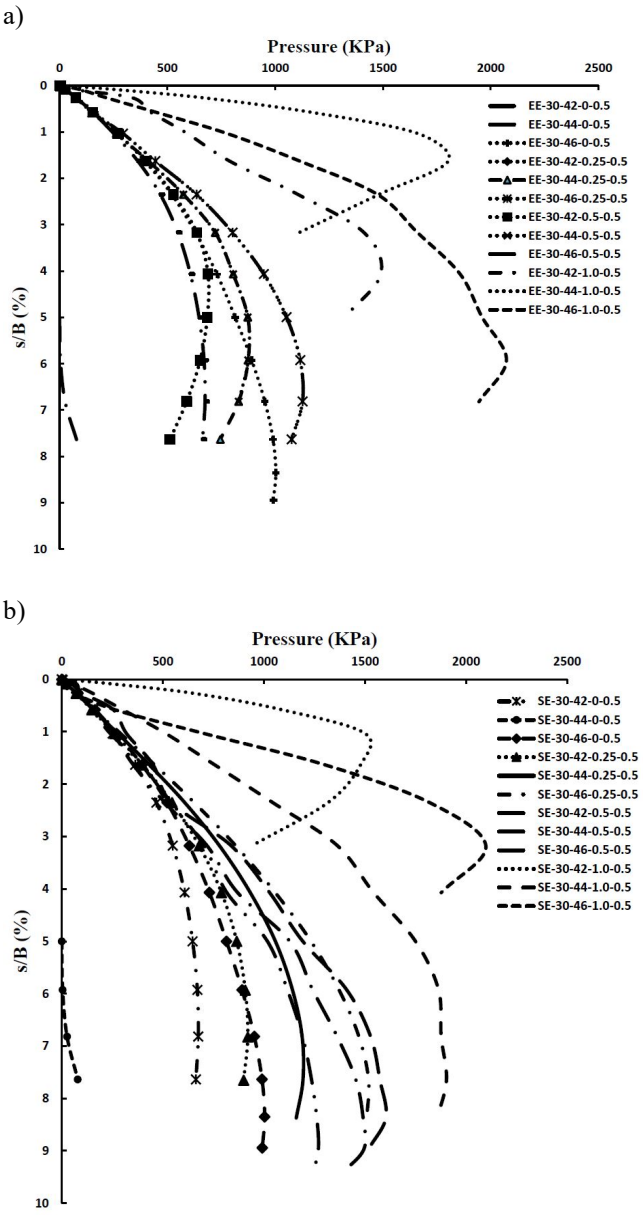

Fig. 4. Pressure settlement ratio plot for the (a) Embedded footing (b) Skirted footing on layered sand at φ_1 =30° and φ_2 = 42°, 44°, 46° corresponding to different D_s/B ratio and at a H/B ratio of 0.5

carried out by varying the embedment and skirt depth in case of embedded and skirted E-shaped footing respectively as 0B to 1B. The thickness and the friction angle of the upper loose sand layer varied from 0.5B to 4B and 30° to 34° respectively. The friction angle of the lower dense sand layer was varied from 42° to 46°. The pressure settlement ratio plots obtained from the numerical study are shown in Figure

4. Figure 4 reveals that with the increase in the friction angle of the lower dense sand layer, the ultimate bearing capacity increased corresponding to a constant friction angle of the upper loose sand layer. Likewise, with the increase in friction angle of upper loose sand layer, the ultimate bearing capacity increased corresponding to a constant friction angle of the lower dense sand layer. In general, with the increase in the friction angle of upper loose or lower dense sand layer results in increase in the ultimate bearing capacity for both the embedded and the skirted footing. However, the increase was higher in case of skirted footing in comparison to the embedded footing. These observations are in agreement with [2,29,37] where the study was conducted using conventional shaped footings. This can be attributed to the fact that the skirt generates additional shear stresses at the skirt-sand interface resulting in higher ultimate bearing capacity of the former.

6.1. Effect of H/B on dimensionless ultimate bearing capacity

To study the effect of thickness of the upper loose sand layer on the dimensionless bearing capacity ($q_u/\gamma_1 B$), the results are presented in Figures 5-7 and the dimensionless bearing capacity values are tabulated in Tables 3 and 4. Study of these figures reveals that for the skirted and embedded E-shaped footing, the dimensionless bearing capacity decreased with the increase in the H/B ratio. This is attributed to the fact that the effect of vertical load diminishes or becomes negligible beyond a depth of 2B for different shapes of footing as per [16]. Further, study of these figures reveals that the decrease in the dimensionless bearing capacity was appreciable up to H/B ratio of 2. Beyond this, the change in the dimensionless bearing capacity was marginal indicating almost negligible contribution of the lower dense sand layer. The above-mentioned trend was similar for all combinations of friction angle of lower and upper sand layers with the increase in the H/B ratio.

Comparison

The comparison of the results obtained from the numerical study for the skirted and embedded E shaped footing, as evident from Table 3 and Table 4, reveals that corresponding to the same H/B ratio, D_s/B ratio and friction angle of the upper loose sand layer, the dimensionless bearing capacity in case of skirted E-shaped footing was higher in comparison to the embedded E-shaped footing.

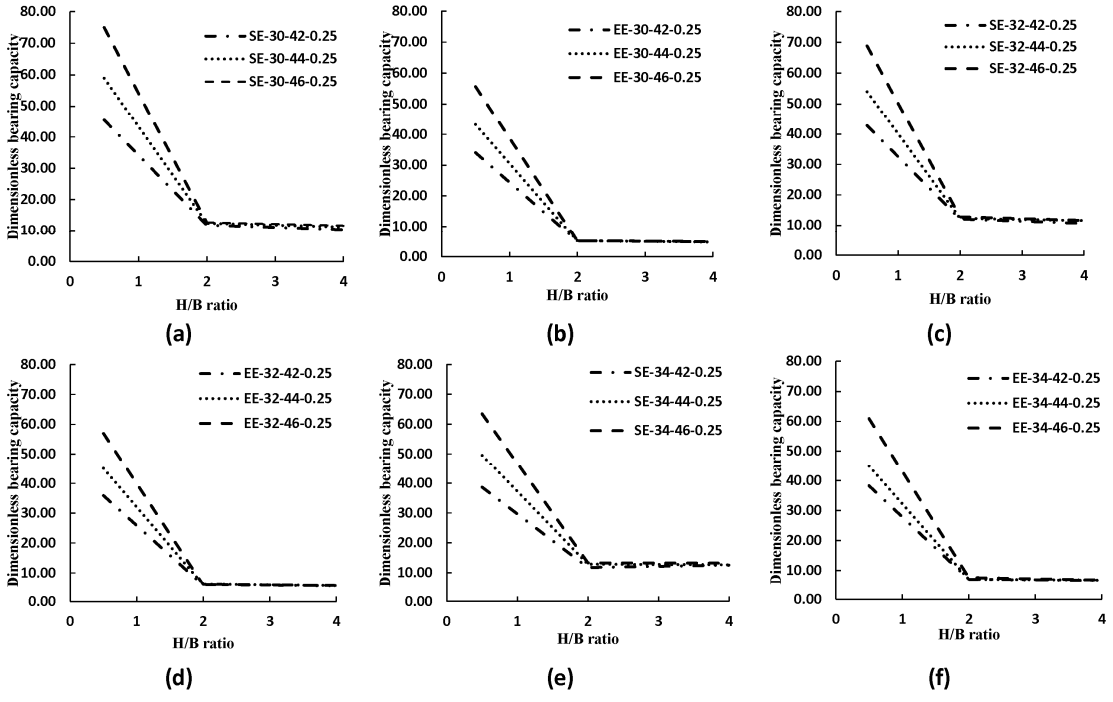

Fig. 5. Variation of dimensional ultimate bearing capacity with the H/B ratio for φ_1 =30°,32°, 34° for the E-shaped embedded (b,d,f), skirted (a, c, e) footing at D_s/B ratio of 0.25

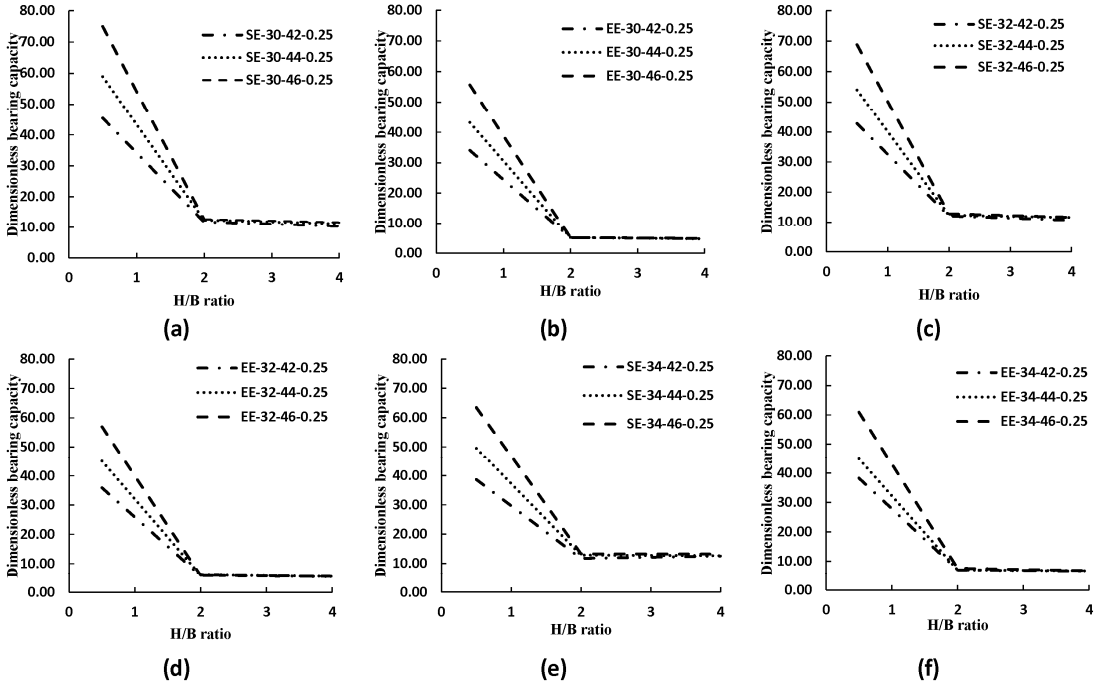

Fig. 6. Variation of dimensional ultimate bearing capacity with the H/B ratio for φ_1 =30°,32°, 34° for the E-shaped embedded (b,d,f), skirted (a,c,e) footing at D_s/B ratio of 0.5

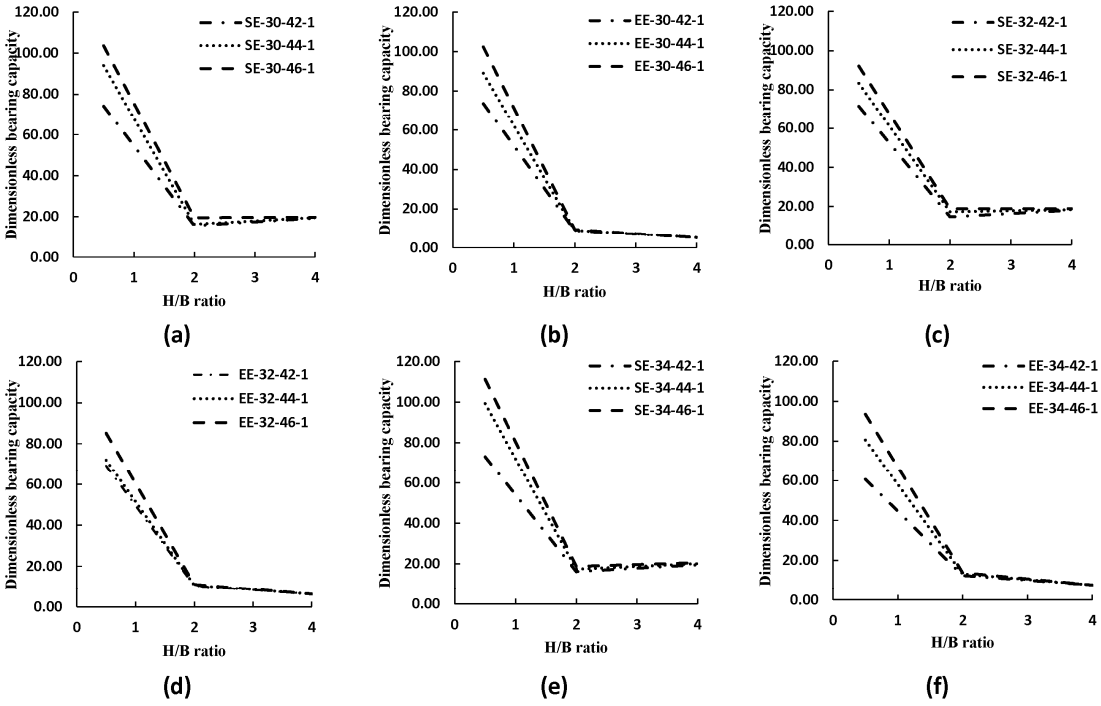

Fig. 7. Variation of dimensional ultimate bearing capacity with the H/B ratio for φ_1 =30°,32°, 34° for the E-shaped embedded (b,d,f), skirted (a,c,e) footing at D_s/B ratio of 1.0

The percentage improvement in the dimension less bearing capacity was tabulated in Table 5. Study of this table reveals that the percentage improvement in the dimensionless bearing capacity was in the range of 0.31% to 61.13%, 30.5% to 146.31% and 73.26% to 282.38% corresponding to H/B ratios of 0.5, 2 and 4 respectively. This table further reveals that the highest increase (283.38%) was observed at a ϕ_1=30° and ϕ_2= 46° at a H/B ratio of 4.0 and Ds/B ratio of 1.0 while the lowest increase (0.31%) was observed at a ϕ_1=34° and ϕ_2= 46° at a H/B ratio of 0.5 and D_s/B ratio of 0.5. The higher improvement in the dimensionless bearing capacity in case of skirted E shaped footing in comparison to the embedded E-shaped footing was in agreement with the literature [2, 29] where the strip and circular footing resting on single layer of sand was investigated.

6.2. Effect of D_s/B on dimensionless ultimate bearing capacity

To study the effect of skirt/embedment depth on the dimensionless bearing capacity ($q_u/\gamma_1 B$), the results are presented in Figures 8-10. Study of these figures reveals that for the embedded and skirted E-shaped footing, the dimensionless bearing capacity increased with the increase in the D_s/B ratio. This is attributed to the fact that failure surfaces generated were contained within the sand layer and could not reach to the surface. The results were in agreement with the earlier studies conducted on different shapes of the multi-edge skirted footings [36-43] resting on single layer of sand. Further study of these figures reveals that the increase in the dimensionless bearing capacity was appreciable for the skirted footing in comparison to the embedded footing.

Table 3.
Dimensionless bearing capacity of skirted E-shaped footing

ϕ_1, ϕ_2	H/B	Bearing capacity ($q_u/\gamma_1 B$) of the skirted E-shaped footing			
		Skirt depth (D_S)			
		0B	0.25B	0.5B	1B
30°,42°	0.5	33.33	45.43	62.69	74.13
30°,44°		41.57	58.91	73.85	93.98
30°,46°		49.55	74.95	79.19	103.59
32°,42°		35.47	42.75	62.55	71.46
32°,44°		44.85	53.97	70.94	83.25
32°,46°		53.15	68.86	77.01	92.08
34°,42°		34.28	38.64	61.60	73.02
34°,44°		44.43	49.49	69.30	99.26
34°,46°		58.10	63.45	75.84	111.23
30°,42°	2.0	4.81	11.76	12.00	15.62
30°,44°		4.92	12.40	12.99	16.31
30°,46°		4.87	12.64	13.18	19.53
32°,42°		5.81	12.07	12.59	14.60
32°,44°		5.78	12.29	12.96	17.20
32°,46°		5.85	12.80	13.14	18.75
34°,42°		7.00	11.73	12.85	16.16
34°,44°		6.95	12.85	14.12	17.37
34°,46°		7.26	13.32	14.98	18.76
30°,42°	4.0	4.20	10.33	10.88	19.30
30°,44°		4.21	11.17	11.44	19.59
30°,46°		4.23	11.60	11.61	19.80
32°,42°		5.08	10.64	10.65	17.97
32°,44°		5.08	11.57	11.69	18.24
32°,46°		5.09	11.62	12.34	18.78
34°,42°		6.42	12.57	12.84	19.56
34°,44°		6.40	12.65	12.89	20.13
34°,46°		6.39	13.17	16.22	20.57

Table 4.
Dimensionless bearing capacity of the embedded E-shaped footing

ϕ1, ϕ2	H/B	Bearing capacity ($q_u/\gamma_1 B$) of the embedded E-shaped footing			
		Embedment depth (D_s)			
		0B	0.25B	0.5B	1B
30°,42°	0.5	33.33	34.02	38.91	73.60
30°,44°		41.57	43.21	49.96	89.04
30°,46°		49.55	55.67	64.85	102.38
32°,42°		35.47	35.87	43.32	69.15
32°,44°		44.85	45.06	55.56	71.94
32°,46°		53.15	56.94	71.61	85.12
34°,42°		34.28	38.26	46.11	60.70
34°,44°		44.43	44.88	59.91	80.58
34°,46°		58.10	60.89	75.60	93.49
30°,42°	2.0	4.81	5.16	5.20	8.81
30°,44°		4.92	5.17	5.31	9.01
30°,46°		4.87	5.19	5.35	9.40
32°,42°		5.81	5.86	6.36	10.25
32°,44°		5.78	5.94	6.40	10.68
32°,46°		5.85	5.89	6.42	10.99
34°,42°		7.00	7.06	7.53	12.38
34°,44°		6.95	7.03	7.96	13.14
34°,46°		7.26	7.60	8.41	13.82
30°,42°	4.0	4.20	4.82	4.76	5.18
30°,44°		4.21	4.74	4.88	5.21
30°,46°		4.23	4.89	4.86	5.18
32°,42°		5.08	5.39	5.73	6.19
32°,44°		5.08	5.46	5.77	6.17
32°,46°		5.09	5.45	5.77	6.21
34°,42°		6.42	6.66	7.41	7.66
34°,44°		6.40	6.78	7.27	7.62
34°,46°		6.39	6.80	7.19	7.63

Table 5
Percentage improvement in the dimensionless bearing capacity

ϕ_1, ϕ_2	H/B	Percentage improvement		
		Skirt/embedment depth (D_s)		
		0.25B	0.5B	1B
30°,42°	0.5	33.56	61.13	0.72
30°,44°		36.33	47.80	5.54
30°,46°		34.64	22.11	1.18
32°,42°		19.16	44.36	3.34
32°,44°		19.77	27.67	15.73
32°,46°		20.92	7.53	8.17
34°,42°		0.99	33.59	20.29
34°,44°		10.28	15.67	23.18
34°,46°		4.21	0.31	18.97

ϕ_1, ϕ_2	H/B	Percentage improvement		
		Skirt/embedment depth (D_s)		
		0.25B	0.5B	1B
30°,42°	2.0	127.95	130.59	77.23
30°,44°		139.63	144.85	81.05
30°,46°		143.63	146.31	107.65
32°,42°		106.04	97.93	42.45
32°,44°		107.01	102.50	60.96
32°,46°		117.20	104.84	70.59
34°,42°		66.30	70.50	30.50
34°,44°		82.63	77.43	32.18
34°,46°		75.22	78.28	35.71
30°,42°	4.0	114.17	128.29	272.91
30°,44°		135.46	134.56	276.09
30°,46°		137.17	138.65	282.38
32°,42°		97.41	85.95	190.20
32°,44°		111.73	102.78	195.58
32°,46°		112.97	113.98	202.22
34°,42°		88.74	73.26	155.47
34°,44°		86.75	77.47	164.02
34°,46°		93.73	125.47	169.72

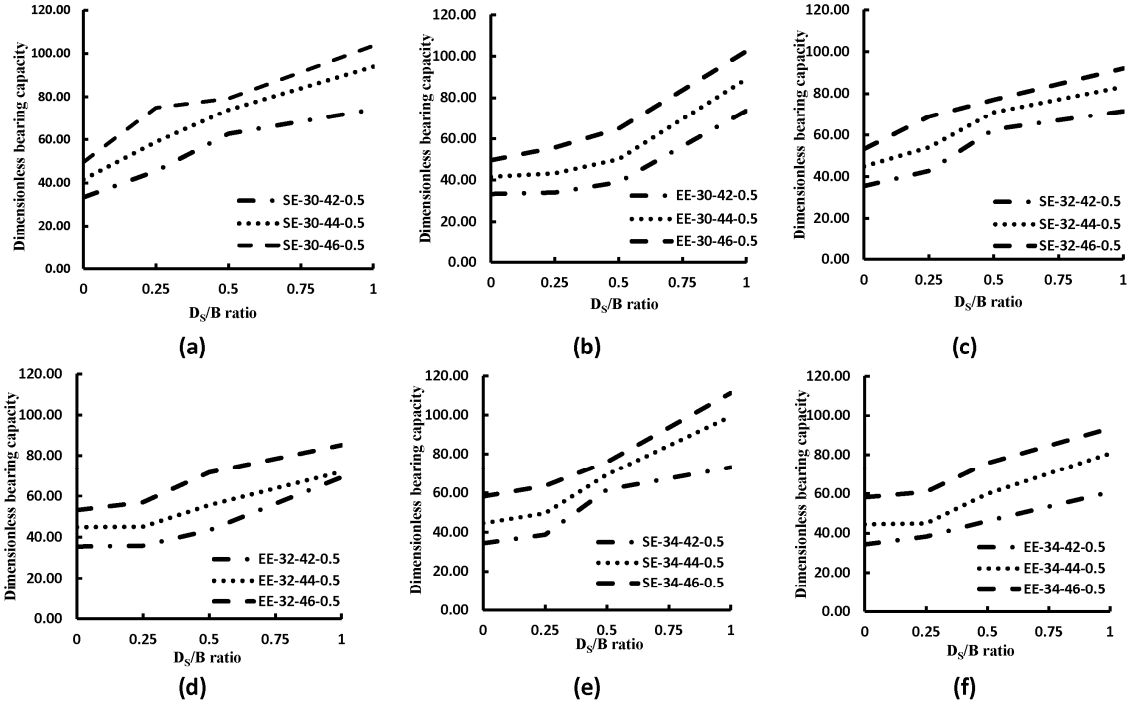

Fig. 8. Variation of dimensional ultimate bearing capacity with the D_s/B ratio for φ_1 =30°,32°, 34° for the E-shaped embedded (b,d,f), skirted (a,c,e) footing at H/B ratio of 0.5

This can be attributed to the additional shear stresses generated at the skirt-sand interface. Similar trend was observed for all combinations of friction angle of lower and upper sand layers and with the increase in the D_s/B ratio.

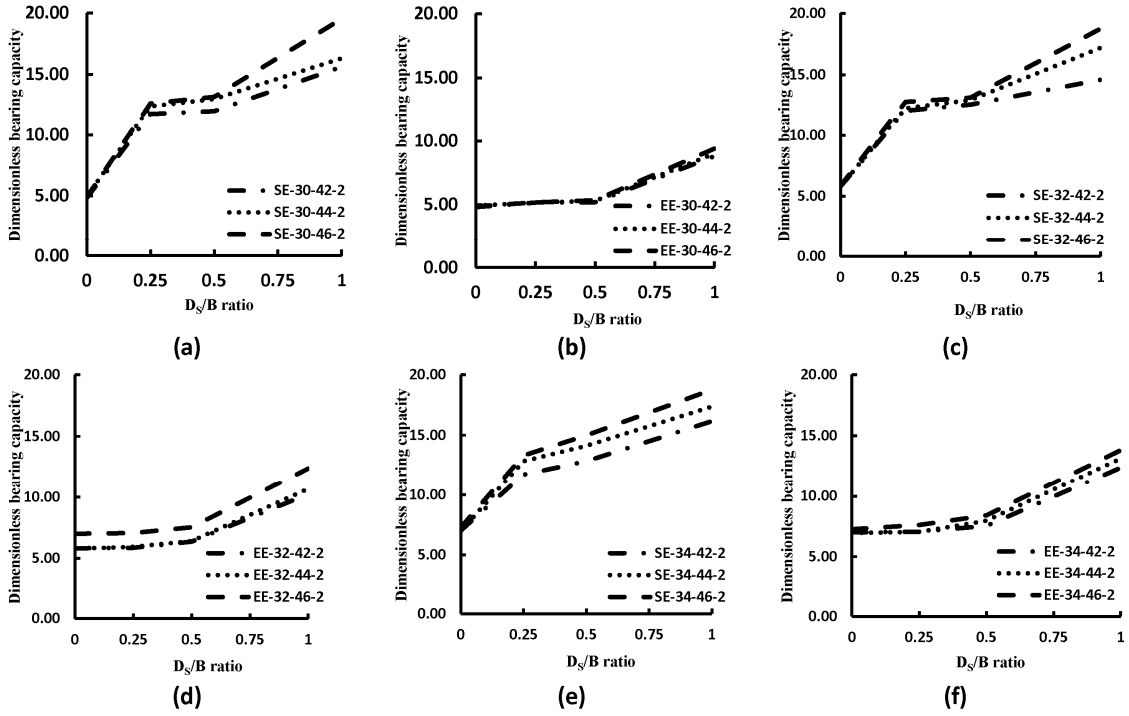

Fig. 9. Variation of dimensional ultimate bearing capacity with the D_s/B ratio for φ_1 =30°, 32°, 34° for the E-shaped embedded (b,d,f), skirted (a, c, e) footing at H/B ratio of 2.0

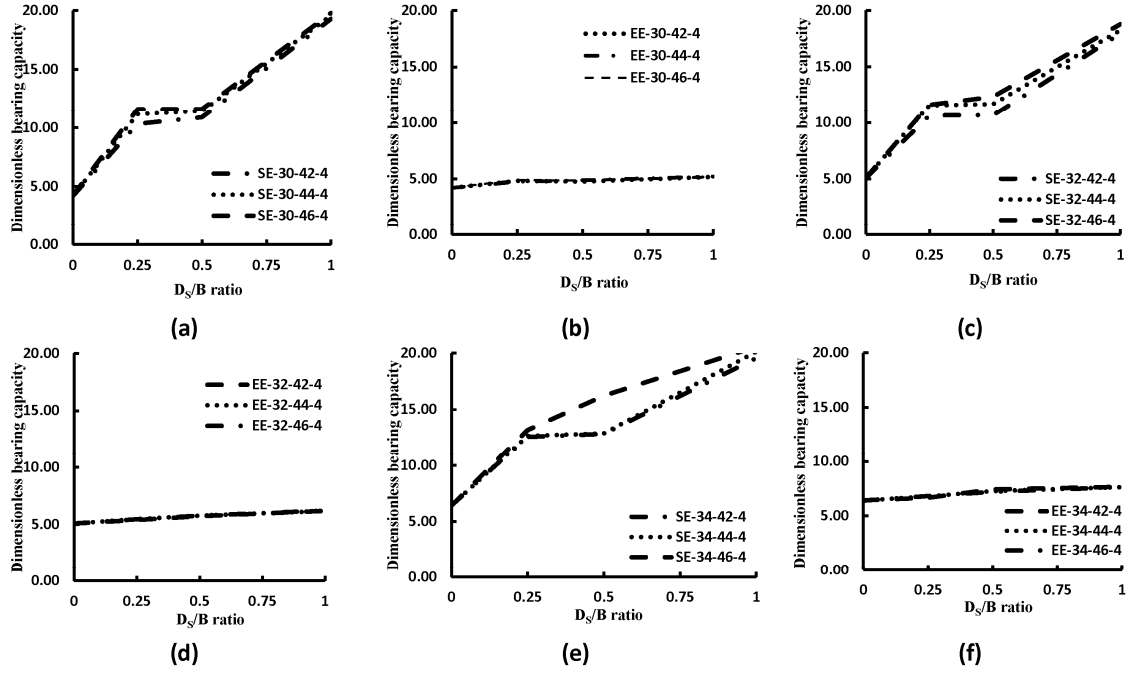

Fig. 10. Variation of dimensional ultimate bearing capacity with the D_s/B ratio for φ_1 =30°, 32°, 34° for the E-shaped embedded (b,d,f), skirted (a, c, e) footing at H/B ratio of 4.0

6.3. Corelation of bearing capacity of skirted footing with the unskirted footing, skirt skin and tip resistance

In order to correlate the bearing capacity of the skirted footing with the bearing capacity of unskirted footing, the skirt skin resistance and tip resistance, it was required to calculate the skin and the tip resistance of the skirt. The skin and tip resistance due to the presence of skirts was calculated by subtracting the bearing capacity of the embedded footing from the bearing capacity of the skirted footing. The authors of this paper believe that the bearing capacity of the skirted footing must be equal the sum of bearing capacity of the surface footing, the skin resistance developed around the skirt surfaces and tip resistance of the skirt. In order to validate this hypothesis, the calculations of the bearing capacity, skin and tip resistance at varying H/B, D_s/B and ϕ_1/ϕ_2 ratio were tabulated in Table 6. In this table Col (4), Col (5), Col (6) and Col (7) shows the bearing capacity of surface, skirted, embedded and skin plus tip resistance of the E shaped footing at varying H/B, D_s/B and ϕ_1/ϕ_2 ratio.

Table 6.
Bearing capacity, skin and tip resistance for at varying H/B, D_s/B and ϕ_1/ϕ_2 ratio

H/B	D_s/B	$\phi 1/\phi 2$	Bearing capacity, skin and tip resistance (kPa) for the E shaped footing				
			Surface	Skirted	Embedded	Skin + tip resistance	Calculated skirted
Col (1)	Col (2)	Col (3)	Col (4)	Col (5)	Col (6)	Col (7)	Col (8)
0.5	0.25	0.71	675.02	920.06	688.86	231.20	906.22
0.5	0.25	0.68	841.85	1192.96	875.04	317.92	1159.77
0.5	0.25	0.65	1003.45	1517.74	1127.29	390.45	1393.90
0.5	0.25	0.76	771.38	929.75	680.25	249.50	1020.88
0.5	0.25	0.73	975.57	1173.86	870.09	303.77	1279.34
0.5	0.25	0.70	1155.91	1497.71	1138.55	359.16	1515.07
0.5	0.25	0.81	771.35	869.44	660.92	208.53	979.88
0.5	0.25	0.77	999.77	1113.51	899.75	213.76	1213.53
0.5	0.25	0.74	1307.26	1427.69	1170.00	257.69	1564.95
0.5	0.5	0.71	675.02	1269.47	787.83	481.64	1156.66
0.5	0.5	0.68	841.85	1495.39	1011.73	483.66	1325.50
0.5	0.5	0.65	1003.45	1603.69	1313.28	290.41	1293.86
0.5	0.5	0.76	771.38	1360.37	942.31	418.06	1189.44
0.5	0.5	0.73	975.57	1542.93	1208.49	334.44	1310.00
0.5	0.5	0.70	1155.91	1674.87	1557.59	117.28	1273.19
0.5	0.5	0.81	771.35	1385.91	1037.46	348.45	1119.80
0.5	0.5	0.77	999.77	1559.27	1348.07	211.20	1210.97
0.5	0.5	0.74	1307.26	1706.36	1701.05	5.31	1312.57
0.5	1.0	0.71	675.02	1501.18	1490.49	10.69	685.72
0.5	1.0	0.68	841.85	1903.03	1803.09	99.94	941.78
0.5	1.0	0.65	1003.45	2097.77	2073.29	24.48	1027.93
0.5	1.0	0.76	771.38	1554.26	1504.00	50.26	821.64
0.5	1.0	0.73	975.57	1810.77	1564.59	246.18	1221.75
0.5	1.0	0.70	1155.91	2002.72	1851.38	151.34	1307.25
0.5	1.0	0.81	771.35	1642.90	1365.81	277.09	1048.44
0.5	1.0	0.77	999.77	2233.24	1813.01	420.23	1420.00
0.5	1.0	0.74	1307.26	2502.78	2103.62	399.16	1706.42
2.0	0.25	0.71	137.50	238.20	83.03	155.17	292.67
2.0	0.25	0.68	141.95	251.05	84.49	166.55	308.50
2.0	0.25	0.65	153.50	255.89	84.77	171.12	324.62
2.0	0.25	0.76	155.00	262.54	107.16	155.39	310.38
2.0	0.25	0.73	162.80	267.27	107.42	159.85	322.65
2.0	0.25	0.70	163.85	278.36	109.11	169.25	333.10
2.0	0.25	0.81	160.78	264.00	138.27	125.73	286.51

H/B	D_s/B	ϕ1/ ϕ2	Bearing capacity, skin and tip resistance (kPa) for the E shaped footing				
			Surface	Skirted	Embedded	Skin + tip resistance	Calculated skirted
Col (1)	Col (2)	Col (3)	Col (4)	Col (5)	Col (6)	Col (7)	Col (8)
2.0	0.25	0.77	163.02	289.05	138.75	150.30	313.32
2.0	0.25	0.74	205.47	299.69	141.04	158.65	364.12
2.0	0.5	0.71	137.50	243.00	85.38	157.61	295.11
2.0	0.5	0.68	141.95	243.11	87.46	155.65	297.60
2.0	0.5	0.65	153.50	246.81	87.32	159.49	312.98
2.0	0.5	0.76	155.00	273.73	114.30	159.43	314.43
2.0	0.5	0.73	162.80	281.50	114.15	167.35	330.15
2.0	0.5	0.70	163.85	285.86	114.56	171.31	335.16
2.0	0.5	0.81	160.78	289.05	149.53	139.52	300.30
2.0	0.5	0.77	163.02	317.80	149.12	168.68	331.70
2.0	0.5	0.74	205.47	337.15	149.12	188.03	393.50
2.0	1.0	0.71	137.50	316.23	178.43	137.80	275.30
2.0	1.0	0.68	141.95	330.32	182.44	147.88	289.82
2.0	1.0	0.65	153.50	395.38	190.41	204.97	358.47
2.0	1.0	0.76	155.00	317.56	222.92	94.64	249.64
2.0	1.0	0.73	162.80	374.02	232.36	141.66	304.46
2.0	1.0	0.70	163.85	407.85	239.08	168.78	332.63
2.0	1.0	0.81	160.78	363.63	278.64	84.99	245.78
2.0	1.0	0.77	163.02	390.78	295.64	95.14	258.15
2.0	1.0	0.74	205.47	422.10	311.04	111.06	316.53
4.0	0.25	0.71	89.88	209.11	96.02	113.08	202.97
4.0	0.25	0.68	92.68	226.09	97.64	128.46	221.13
4.0	0.25	0.65	112.55	234.93	99.06	135.87	248.43
4.0	0.25	0.76	92.86	231.39	116.83	114.55	207.41
4.0	0.25	0.73	102.50	251.61	117.21	134.40	236.90
4.0	0.25	0.70	113.76	252.66	118.83	133.83	247.59
4.0	0.25	0.81	150.55	282.36	149.85	132.50	283.05
4.0	0.25	0.77	155.19	284.68	152.44	132.24	287.43
4.0	0.25	0.74	190.32	296.44	153.02	143.42	333.74
4.0	0.5	0.71	89.88	220.26	96.48	123.78	213.66
4.0	0.5	0.68	92.68	231.69	98.52	133.18	225.85
4.0	0.5	0.65	112.55	233.11	98.78	134.33	246.89
4.0	0.5	0.76	92.86	231.69	124.59	107.09	199.95
4.0	0.5	0.73	102.50	244.28	125.40	118.88	221.38
4.0	0.5	0.70	113.76	238.33	125.40	112.93	226.69
4.0	0.5	0.81	150.55	279.01	161.87	117.14	267.69
4.0	0.5	0.77	155.19	287.12	163.48	123.65	278.84
4.0	0.5	0.74	190.32	364.96	166.81	198.15	388.47
4.0	1.0	0.71	89.88	209.11	104.80	104.31	194.19
4.0	1.0	0.68	92.68	226.09	104.84	121.26	213.93
4.0	1.0	0.65	112.55	234.93	105.50	129.43	241.98
4.0	1.0	0.76	92.86	231.39	134.24	97.15	190.00
4.0	1.0	0.73	102.50	251.61	134.67	116.95	219.44
4.0	1.0	0.70	113.76	252.66	135.17	117.49	231.25
4.0	1.0	0.81	150.55	282.83	171.52	111.31	261.86
4.0	1.0	0.77	155.19	284.68	171.61	113.07	268.26
4.0	1.0	0.74	190.32	296.44	172.25	124.19	314.50

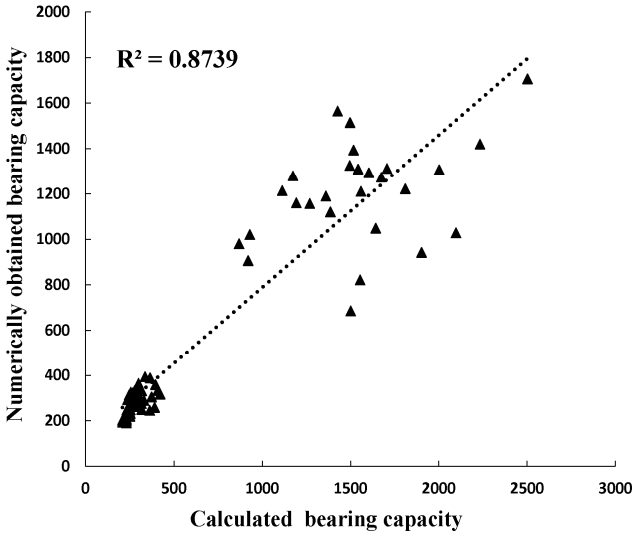

Fig. 11. Plot between calculated and numerically obtained bearing capacity of skirted E shaped footing

The values in Col (7) were obtained by subtracting the values given in Col (6) from the values given in Col (5). The values in Col (8) were obtained by adding the values given in Col (4) and Col (7). The values in column (5) were plotted against the calculated values of bearing capacity of the skirted E shaped footing given in column (8) and the plot is shown in Figure 11. Study of this figure reveals that the statistical coefficient of determination was obtained as 0.8739 which fairly validates the current hypothesis.

6.4. Failure patterns

The typical failure patterns below the embedded and skirted E-shaped footing at ϕ_1 = 30° and ϕ_2 = 42° corresponding to H/B ratio of 4.0 and a D_s/B ratio of 0. 5 is presented in Figure 12. Study of this figure reveals that with the provision of skirt or placing the footing at a certain depth below the ground level intercepts the failure patterns. A close examination of this figure further reveals that higher yielding of layered sand occurred in case of skirted E-shaped footing in comparison to the embedded E-shaped footing. Moreover, the plastic strain observed was similar at all the sections of the skirted E-shaped footing. It can be further inferred from this figure that similar mode of failure was observed with both (skirted as well as embedded E-shaped) the footings on layered sand with no occurrence of heave at the ground surface in all the case combinations studied. The only difference observed in the behaviour of both the footings was the lateral spread of the failure surface along the width. For the skirted E-shaped footing, the lateral spread was more as in comparison to the embedded E-shaped footing. However, the lateral spread was confined below the skirt tip level (in case skirted footing) and beneath

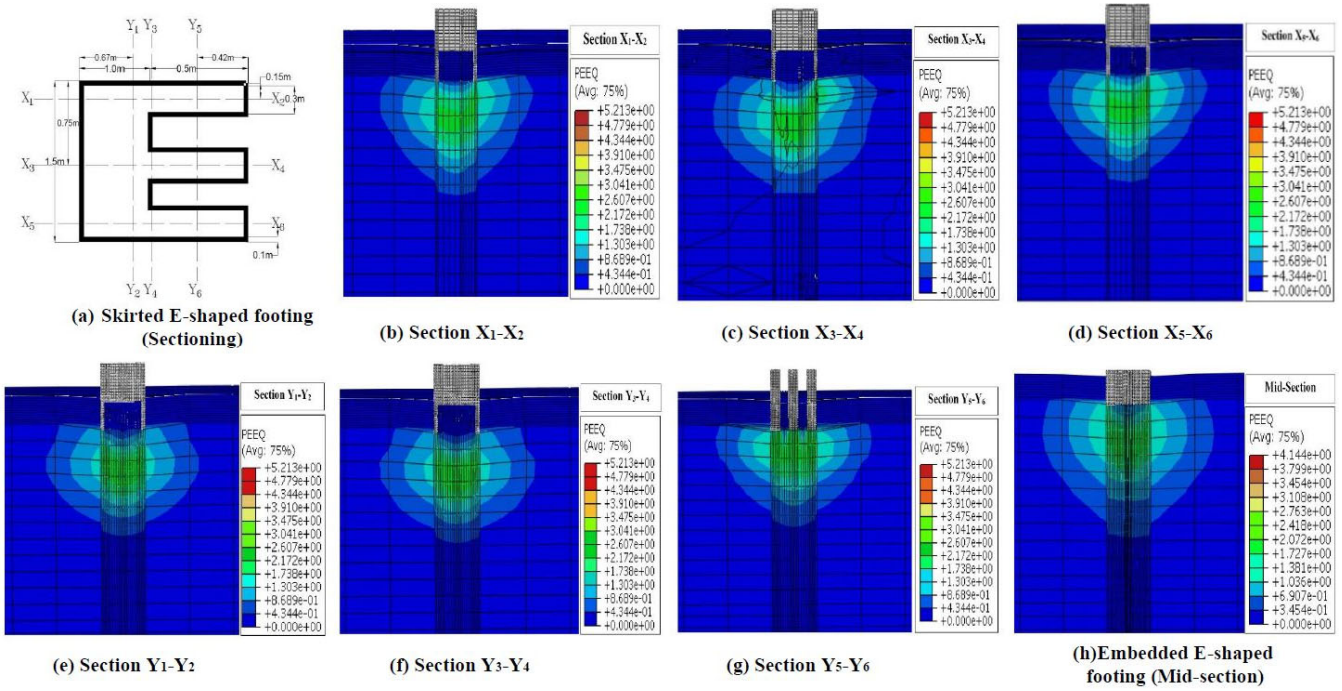

Fig. 12. Failure pattern below the skirted and embedded footing at D_s/B ratio 0.5 and for φ_1 =30° and φ_2 =42° at H/B ratio of 4.0

the base of the embedded footing respectively. In addition, as shown in Figure 12, section Y_5-Y_6 showed interference of the E-shaped footing's cantilever arm with the failure surface reaching the tip of the skirt at the edges of the cantilever arms. This could be attributed to the shape of the skirt and the empty space between the cantilever arms that was filled with foundation sand under the footing, confining the sand in between the surrounding skirt, leading to further stress concentrations in section Y_5-Y_6. However, the overall mode of failure was the local shear failure in all the cases studied both for the skirted and embedded E-shaped footings.

6.5. Displacement contours

Typical displacement contours for the unskirted, skirted and embedded E-shaped footing resting on loose sand layer with ϕ_1=30° overlying dense sand layer with ϕ_2= 42° corresponding to H/B and D_s/B ratio of 4 and 0.25 respectively are presented in Figure 13. This figure depicts the total contour of the displacement and their importance is to assess the actual displacement under the load. This type of information is required to verify the vertical settlement in the footing design within the acceptable limits or not under the load. Analysis of this figure reveals that the maximum displacement was observed immediately below the unskirted and embedded E-shaped footing whereas the maximum displacement occurred at the skirt tip in case of skirted E-shaped footing. This indicates that the behaviour of the skirted E-shaped footing is similar to the one observed for the embedded footing.

In addition, the analysis of this figure indicates that the displacement contours remained well established within the selected lateral and vertical boundaries for the unskirted, skirted and embedded E-shaped footings corresponding to H/B ratios of 0.5, 2 and 4. This means that the horizontal and vertical extent chosen was adequate for the current problem. The knowledge gained from the study of displacement contours will be helpful in developing analytical solutions.

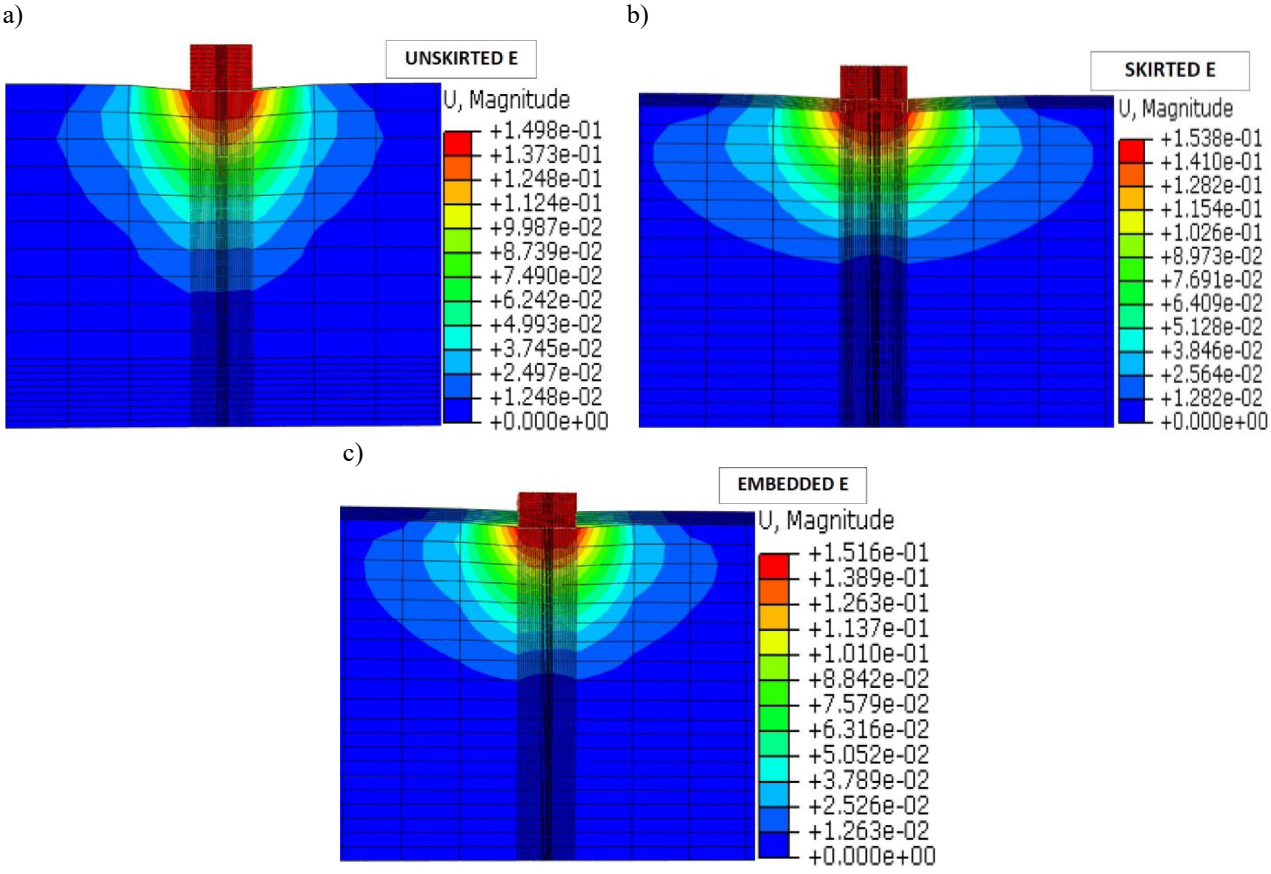

Fig. 13. Displacement contours for the (a) unskirted (b) skirted (c) embedded E-shaped footing corresponding to D_s/B and H/B ratio 0.25 and 4.0 restively for resting on upper loose sand layer with ϕ_1=30° overlying dense sand layer with ϕ_2= 42°

7. Conclusions

The numerical study on the skirted and embedded E-shaped footing resting on upper loose sand overlying lower dense sand layer and subjected to vertical concentric load was investigated. A total of 216 tests using finite element analysis were performed to assess the behaviour. From the results and discussion presented above, the following conclusions are drawn:

1. The ultimate bearing capacity was higher for the skirted E-shaped footing followed by embedded E-shaped footing and unskirted E-shaped footing in this order for all combinations of variables studied.
2. The improvement in the ultimate bearing capacity for the skirted E-shaped footing in comparison to the embedded E-shaped footing was in the range of 0.31% to 61.13%, 30.5% to 146.31% and 73.26% to 282.38% corresponding to H/B ratios of 0.5, 2.0 and 4.0 respectively.
3. The highest increase (283.38 %) was observed at φ_1 =30° and φ_2 =46° corresponding to H/B and D_s/B ratio of 4.0 and 1.0 respectively while the increase was lowest (0.31%) at φ_1 =34° and φ_2 =46° at H/B ratio of 0.5 and D_s/B ratio of 0.5.
4. For the skirted E-shaped footing, the lateral spread was more as in comparison to the embedded E-shaped footing.
5. The bearing capacity of the skirted footing was equal the sum of bearing capacity of the surface footing, the skin resistance developed around the skirt surfaces and tip resistance of the skirt with coefficient of determination as 0.8739.
6. The highest displacement was found below the unskirted and embedded E-shaped footing, and at the skirt tip in the case of the skirted E-shaped footing. Further, the displacement contours generated supports the observations of the multi-edge embedded and skirted footings regarding the ultimate bearing capacity on layered sands.

However, further validation of the results presented in this paper, is recommended using experimental study conducted on similar size embedded and skirted E shaped footing. The proposed numerical study can be an advantage for the architects designing similar types of super structures requiring similar shaped footings.

Acknowledgements

I would like to express my special thanks of gratitude to Central Building Research Institute (CSIR-CBRI) Roorkee for providing me the opportunity to utilize the ABACUS software.

Notations

B	Width of footing
H	Thickness of the upper loose sand layer
s	Settlement of footing
s/B	Normalized settlement
γ_1	Unit weight of upper loose sand layer
γ_2	Unit weight of lower dense sand layer
ϕ_1	Friction angle of upper loose sand
ϕ_2	Friction angle of lower dense sand
μ_1	Poisson ratio of upper loose sand layer
μ_2	Poisson ratio of lower dense sand layer
E_1	Modulus of elasticity of upper loose sand layer
E_2	Modulus of elasticity of lower dense sand layer
Ψ_1	Dilation angle of upper loose sand layer
Ψ_2	Dilation angle of lower dense sand layer
H/B	Thickness ratio
D_s	Skirt or embedment depth
D_s/B	Depth ratio
q_u	Ultimate bearing capacity
$q_u/\gamma_1 B$	Dimensionless ultimate bearing capacity
R^2	Coefficient of determination

References

[1] B. Bienen, C. Gaudin, M.J. Cassidy, L. Rausch, O.A. Purwana, H. Krisdani, Numerical modelling of a hybrid foundation under combined loading, Computers and Geotechnics 45 (2012) 127-139. DOI: https://doi.org/10.1016/j.compgeo.2012.05.009

[2] J. Kumar, V.N. Khatri, A. Kumar, Performance of skirted and embedded circular footing on sand, Proceedings of the 2nd ASCE International Conference, 2020.

[3] S.K. Vanapalli, F.M.O. Mohamed, Bearing capacity and settlement of footings in unsaturated sands, International Journal of GEOMATE 5/1 (2013) 595-604.

[4] Adarsh Thakur, Rakesh Kumar Dutta, A study on bearing capacity of skirted square footings on different sands, Indian Geotechnical Journal 50 (2020) 1057-1073. DOI: https://doi.org/10.1007/s40098-020-00440-4

[5] A.K. Nazir, W.R. Azzam, Improving the bearing capacity of footing on soft clay with sand pile with/without skirts, Alexandria Engineering Journal 49/4 (2010) 371-377. DOI: https://doi.org/10.1016/j.aej.2010.06.002

[6] A.Z. EL Wakil, Horizontal capacity of skirted circular shallow footings on sand, Alexandria Engineering Journal 49/4 (2010) 379-385. DOI: https://doi.org/10.1016/j.aej.2010.07.003

[7] A.Z. EL Wakil, Bearing capacity of Skirt circular footing on sand, Alexandria Engineering Journal 52/3 (2013) 359-364. DOI: https://doi.org/10.1016/j.aej.2013.01.007
[8] H.T. Eid, Bearing capacity and settlement of skirted shallow foundations on sand, International Journal of Geomechanics 13/5 (2013) 645-652. DOI: https://doi.org/10.1061/(ASCE)GM.1943-5622.0000237
[9] H.T. Eid, O.A. Alansari, A.M. Odeh, M.N. Nasr, H.A. Sadek, Comparative study on the behavior of square foundations resting on confined sand, Canadian Geotechnical Journal 46/4 (2009) 438-453. DOI: https://doi.org/10.1139/T08-134
[10] V.N. Khatri, S.P. Debbarma, R.K. Dutta, B. Mohanty, Pressure-settlement behavior of square and rectangular skirted footings resting on sand, Geomechanics and Engineering 12/4 (2017) 689-705. DOI: https://doi.org/10.12989/gae.2017.12.4.689
[11] A.E. Elsaied, N.M. Saleh, M.E. Elmashad, Behavior of Circular Footing resting on Laterally Confined Granular Reinforced Soil, HBRC Journal 11/2 (2015) 240-245. DOI: https://doi.org/10.1016/j.hbrcj.2014.03.011
[12] G. Sajjad, M. Masoud, Study of the behaviour of skirted shallow foundations resting on sand, International Journal of Physical Modelling in Geotechnical Engineering 18/3 (2018) 117-130. DOI: https://doi.org/10.1680/jphmg.16.00079
[13] M.Y. Al-Aghbari, Y.E.-A. Mohamedzein, The use of skirts to improve the performance of a footing on sand, International Journal of Geotechnical Engineering 14/2 (2020) 134-141. DOI: https://doi.org/10.1080/19386362.2018.1429702
[14] M.Y. Al-Aghbari, R.K. Dutta, Performance of square footing with structural skirt resting on sand, Geomechanics and Geoengineering 3/4 (2008) 271-277. DOI: https://doi.org/10.1080/17486020802509393
[15] M.Y. Al-Aghbari, Settlement of shallow circular foundations with structural skirts resting on sand, The Journal of Engineering Research [TJER] 4/1 (2007) 11-16. DOI: https://doi.org/10.24200/tjer.vol4iss1pp11-16
[16] A.M. Hanna, Finite element analysis of footings on layered soils, Mathematical Modelling 9/11 (1987) 813-819. DOI: https://doi.org/10.1016/0270-0255(87)90501-X
[17] A.M. Hanna, Bearing capacity of foundations on a weak sand layer overlying a strong deposit, Canadian Geotechnical Journal 19/3 (1982) 392-396. DOI: https://doi.org/10.1139/t82-043
[18] A. Mosadegh, H. Nikraz, Bearing capacity evaluation of footing on a layered-soil using ABAQUS, Journal of Earth Science & Climatic Change 6/3 (2015) 264. DOI: https://doi.org/10.4172/2157-7617.1000264
[19] A. Gupta, R.K. Dutta, R. Shrivastava, Ultimate bearing capacity of square/rectangular footing on layered soil, Indian Geotechnical Journal 47/3 (2017) 303-313. DOI: https://doi.org/10.1007/s40098-017-0233-y
[20] G.G. Meyerhof, Ultimate bearing capacity of footings on sand layer overlying clay, Canadian Geotechnical Journal 11/2 (1974) 223-229. DOI: https://doi.org/10.1139/t74-018
[21] J.S. Shiau, A.V. Lyamin, S.W. Sloan, Bearing capacity of a sand layer on clay by finite element limit analysis, Canadian Geotechnical Journal 40/5 (2003) 900-915. DOI: https://doi.org/10.1139/t03-042
[22] M. Georgiadis, A. Michalopoulos, Bearing capacity of gravity bases on layered soil, Journal of the Geotechnical Engineering 111/6 (1985) 712-729. DOI: https://doi.org/10.1061/(ASCE)0733-9410(1985)111:6(712)
[23] M.J. Kenny, K.Z. Andrawes, The bearing capacity of footings on a sand layer overlying soft clay, Geotechnique 47/2 (1997) 339-345. DOI: https://doi.org/10.1680/geot.1997.47.2.339
[24] M.D. Shoaei, A. Alkarni, J. Noorzaei, M.S. Jaafar, B.B.K. Huat, Review of available approaches for ultimate bearing capacity of two-layered soils, Journal of Civil Engineering and Management 18/4 (2012) 469-482. DOI: https://doi.org/10.3846/13923730.2012.699930
[25] V. Panwar, R.K. Dutta, Numerical study of ultimate bearing capacity of rectangular footing on layered sand, Journal of Achievements in Materials and Manufacturing Engineering 101/1 (2020) 15-26. DOI: https://doi.org/10.5604/01.3001.0014.4087
[26] Z. Szypcio, K. Dołżyk, The bearing capacity of layered subsoil, Studia Geotechnica et Mechanica XXVIII/1 (2006) 45-60.
[27] P.P. Das, V.N. Khatri, R.K. Dutta, Bearing capacity of ring footing on weak sand layer overlying a dense sand deposit, Geomechanics and Geoengineering 16/4 (2021) 249-262. DOI: https://doi.org/10.1080/17486025.2019.1664775
[28] Y. Hu, M.F. Randolph, P.G. Watson, Bearing capacity response of skirted foundation on non-homogenous soils, Journal of Geotechnical and Geoenvironmental Engineering 125/11 (1999) 924-935. DOI: https://doi.org/10.1061/(ASCE)1090-0241(1999)125:11(924)

[29] V.N. Khatri, J. Kumar, Finite-element limit analysis of strip and circular skirted footings on sand, International Journal of Geomechanics 19/3 (2019). DOI: https://doi.org/10.1061/(ASCE)GM.1943-5622.0001370
[30] M. Laman, A. Yildiz, Numerical studies of ring foundations on geogrid-reinforced sand, Geosynthetics International 14/2 (2007) 52-64. DOI: https://doi.org/10.1680/gein.2007.14.2.52
[31] S. Alzabeebee, Dynamic response and design of a skirted strip foundation subjected to vertical vibration, Geomechanics and Engineering 20/4 (2020) 345-358. DOI: https://doi.org/10.12989/gae.2020.20.4.345
[32] Y. Turedi, B. Emirler, M. Ornek, A. Yildiz, Determination of the bearing capacity of model ring footings: experimental and numerical investigations, Geomechanics and Engineering 18/1 (2019) 29-39. DOI: https://doi.org/10.12989/gae.2019.18.1.029
[33] D.R. Phatak, D.J. Khamkar, E.A. Dickin, R. Nazir, Moment-carrying capacity of short pile foundations in cohesionless soil, Journal of Geotechnical and Geoenvironmental Engineering 125/1 (1999) 1-10. DOI: https://doi.org/10.1061/(ASCE)1090-0241(2000)126:6(581)
[34] J. Li, Y. Tian, M.J. Cassidy, Failure mechanism and bearing capacity of footings buried at various depths in spatially random soil, Journal of Geotechnical and Geoenvironmental Engineering 141/2 (2015) 04014099. DOI: https://doi.org/10.1061/(ASCE)GT.1943-5606.0001219
[35] V.C. Joshi, R.K. Dutta, R. Shrivastava, Ultimate bearing capacity of circular footing on layered soil, Journal of Geoengineering 10/1 (2015) 25-34. DOI: http://dx.doi.org/10.6310/jog.2015.10(1).4
[36] T. Gnananandarao, R.K. Dutta, V.N. Khatri, Model studies of plus and double box shaped skirted footings resting on sand, International Journal of Geo-Engineering 11 (2020) 2. DOI: https://doi.org/10.1186/s40703-020-00109-0
[37] T. Gnananandarao, V.N. Khatri, R.K. Dutta, Performance of multi-edge skirted footings resting on sand, Indian Geotechnical Journal 48 (2018) 510-519. DOI: https://doi.org/10.1007/s40098-017-0270-6
[38] A. Thakur, R.K. Dutta, Experimental and numerical studies of skirted hexagonal footings on three sands, SN Applied Sciences 2 (2020) 487. DOI: https://doi.org/10.1007/s42452-020-2239-9
[39] T. Gnananandarao, V.N. Khatri, R.K. Dutta, Pressure settlement ratio behavior of plus shaped skirted footing on sand, Journal of Civil Engineering (IEB) 46/2 (2018) 161-170.
[40] B. Davarci, M. Ornek, Y. Turedi, Model studies of multi-edge footings on geogrid-reinforced sand, European Journal of Environmental and Civil Engineering 18/2 (2014) 190-205. DOI: https://doi.org/10.1080/19648189.2013.854726
[41] B. Davarci, M. Ornek, Y. Turedi, Analyses of multi-edge footings rested on loose and dense sand, Civil Engineering 58/4 (2014) 355-370. DOI: https://doi.org/10.3311/PPci.2101
[42] M. Ghazavi, H. Mirzaeifar, Bearing capacity of multi-edge shallow foundations on geogrid-reinforced sand, Proceedings of the 4th International Conference on Geotechnical Engineering and Soil Mechanics, Tehran, Iran, 2010, 1-9.
[43] A. Thakur, R.K. Dutta, A study of bearing capacity of skirted octagonal footings resting on different sands, Archives of Materials Science and Engineering 107/1 (2021) 21-31. DOI: https://doi.org/10.5604/01.3001.0014.8191
[44] S. Keawsawasvong, C. Thongchom, S. Likitlersuang, Bearing capacity of strip footing on Hoek-brown rock mass subjected to eccentric and inclined loading, Transportation Infrastructure Geotechnology 8/1 (2021) 189-202. DOI: https://doi.org/10.1007/s40515-020-00133-8
[45] S. Keawsawasvong, V.Q. Lai, End bearing capacity factor for annular foundations embedded in clay considering the effect of the adhesion factor, International Journal of Geosynthetics and Ground Engineering 7 (2021) 15. DOI: https://doi.org/10.1007/s40891-021-00261-2
[46] B. Ukritchon, S. Keawsawasvong, Undrained lower bound solutions for end bearing capacity of shallow circular piles in non-homogenous and anisotropic clays, International Journal for Numerical and Analytical Methods in Geomechanics 44/5 (2020) 596-632. DOI: https://doi.org/10.1002/nag.3018
[47] B. Ukritchon, S. Yoang, S. Keawsawasvong, Bearing capacity of shallow foundations in clay with linear increase in strength and adhesion factor, Marine Georesources and Geotechnology 36/4 (2018) 438-451. DOI: https://doi.org/10.1080/1064119X.2017.1326991
[48] B. Ukritchon, S. Keawsawasvong, Unsafe error in conventional shape factor for shallow circular foundations in normally consolidated clays, Journal of Geotechnical and Geoenvironmental Engineering 143/6 (2017) 02817001. DOI: https://doi.org/10.1061/(ASCE)GT.1943-5606.0001670

[49] B. Ukritchon, J.C. Faustino, S. Keawsawasvong, Numerical investigations of pile load distribution of pile group foundation subjected to vertical load and large moment, Geomechanics and Engineering 10/5 (2016) 577-598 DOI: https://doi.org/10.12989/gae.2016.10.5.577
[50] J.E. Bowles, Foundation analysis and design, McGraw-Hill, New York, 1977.
[51] E.-S.A.A. El-Kasaby, Estimation of guide values for the modulus of elasticity of soil, Bulletin of Faculty of Engineering, Assiut University 19/1 (1991) 1-7.
[52] IS 6403, Code of practice for determination of breaking capacity of shallow foundations, Bureau of Indian Standard, New Delhi, India, 1981.
[53] M.D. Bolton, The strength and dilatancy of sands, Geotechnique 36/1 (1986) 65-78. DOI: https://doi.org/10.1680/geot.1986.36.1.65
[54] P. Pal, Dynamic poisson's ratio and modulus of elasticity of pozzolana portland cement concrete, International Journal of Engineering and Technology Innovation 9/2 (2019) 131-144.
[55] IS 456, Indian standard code of practice for plain and reinforced concrete (Fourth Revision), Bureau of Indian Standard, New Delhi, India, 2007.
[56] IS 800, Indian standard for general construction in steel - Code of Practice (Third Revision), Bureau of Indian Standard, New Delhi, India, 2007.